
THERMAL TRANSPORT IN $d = 1, 2, 3$ - A CONSPIRACY ENTHRONING FOURIER LAW [†]

Constantino Tsallis^a, Henrique Santos Lima^b, Ugur Tirnakli^c and Deniz Eroglu^d

“Yo soy yo y mi circunstancia” (Ortega y Gasset)

ABSTRACT

We numerically study the thermal transport in the classical inertial nearest-neighbor XY ferromagnet in $d = 1, 2, 3$, the total number of sites being given by $N = L^d$, where L is the linear size of the system. For the thermal conductivity σ , we obtain $\sigma(T, L)L^{\delta(d)} = A(d)e_{q(d)}^{-B(d)[L^{\gamma(d)}T]^{\eta(d)}}$ (with $e_q^z \equiv [1 + (1 - q)z]^{1/(1-q)}$; $e_1^z = e^z$; $A(d) > 0$; $B(d) > 0$; $q(d) > 1$; $\eta(d) > 2$; $\delta \geq 0$; $\gamma(d) > 0$), for all values of $L^{\gamma(d)}T$ for $d = 1, 2, 3$. In the $L \rightarrow \infty$ limit, we have $\sigma \propto 1/L^{\rho_\sigma(d)}$ with $\rho_\sigma(d) = \delta(d) + \gamma(d)\eta(d)/[q(d) - 1]$. The material conductivity is given by $\kappa = \sigma L^d \propto 1/L^{\rho_\kappa(d)}$ ($L \rightarrow \infty$) with $\rho_\kappa(d) = \rho_\sigma(d) - d$. Our numerical results are consistent with ‘conspiratory’ d -dependences of $(q, \eta, \delta, \gamma)$, which comply with normal thermal conductivity (Fourier law) for all dimensions.

1 Introduction

Heat transport, charge transport and mass diffusive transport are basic nonequilibrium phenomena widely occurring in nature. Their macroscopic behaviors in three-dimensional systems ($d = 3$) are respectively determined by Fourier’s law [1], Ohm’s law [2] and Fick’s laws [3]. The verification of the validity or breakdown for d -dimensional systems provides a deeper understanding of nonequilibrium stationary states in general. A sensible effort has been dedicated in the literature to study the validity or breakdown of Fourier law in both classical and quantum systems of various dimensionalities [4, 5, 6, 7, 8, 9, 10, 11, 12, 13, 14, 15]. Along this line, we focus in the present paper on Fourier law for a paradigmatic $d = 1, 2, 3$ classical model, namely the inertial first-neighbor XY ferromagnet (or planar-rotator model) in d -dimensional hypercubic lattices. The Hamiltonian is given by [17, 19, 16, 18]

$$\mathcal{H} = \frac{1}{2} \sum_{\ell=1}^{L^d} p_\ell^2 + \frac{1}{2} \sum_{\langle \ell, \ell' \rangle} [1 - \cos(\theta_\ell - \theta_{\ell'})], \quad (1)$$

where $\langle \ell, \ell' \rangle$ denotes nearest-neighboring rotors in the d -dimensional lattice. We have considered unit momenta of inertia and unit first-neighbor coupling constant without loss of generality, and (p_ℓ, θ_ℓ) are conjugate canonical pairs. We use periodic boundary conditions along $(d - 1)$ directions, leaving open $(d - 1)$ -dimensional ends, one of them

^a *Centro Brasileiro de Pesquisas Físicas and National Institute of Science and Technology of Complex Systems, Rua Xavier Sigaud 150, Rio de Janeiro-RJ 22290-180, Brazil*
Santa Fe Institute, 1399 Hyde Park Road, Santa Fe, New Mexico 87501, USA
Complexity Science Hub Vienna, Josefstädter Strasse 39, 1080 Vienna, Austria
 E-mail: tsallis@cbpf.br

^b *Centro Brasileiro de Pesquisas Físicas, Rua Xavier Sigaud 150, Rio de Janeiro-RJ 22290-180, Brazil.*
 E-mail: hslima94@cbpf.br

^c *Department of Physics, Faculty of Science, Ege University, 35100 Izmir, Turkey.*
 E-mail: ugur.tirnakli@ege.edu.tr

^d *Faculty of Engineering and Natural Sciences, Kadir Has University, 34083, Istanbul, Turkey*
 E-mail: deniz.eroglu@khas.edu.tr

being at low temperature T_l and the other one at high temperature T_h . The model is then defined as an L -sized open chain for $d = 1$ with two ending sites at its borders, an $(L \times L)$ -sized cylindrical tube for $d = 2$ with two L -sized circular rings at its borders, and an $(L \times L \times L)$ -sized torus for $d = 3$ with two circular plaquettes at its two ends along the open direction. We note $T \equiv (T_h + T_l)/2$ the average temperature.

2 Results

The equations of motion for the d -dimensional model are the following ones.

For $d = 1$ (see Fig. 1):

$$\begin{aligned}\dot{\theta}_i &= p_i \quad (i = 1, \dots, L) \\ \dot{p}_1 &= -\gamma_h p_1 + F_1 + \sqrt{2\gamma_h T_h} \eta_h(t) \\ \dot{p}_i &= F_i \quad (i = 2, \dots, L-1) \\ \dot{p}_L &= -\gamma_l p_L + F_L + \sqrt{2\gamma_l T_l} \eta_l(t),\end{aligned}\tag{2}$$

the force components being given by

$$\begin{aligned}F_1 &= -\sin(\theta_1 - \theta_2) - \sin(\theta_1) \\ F_i &= -\sin(\theta_i - \theta_{i+1}) - \sin(\theta_i - \theta_{i-1}) \quad (i = 2, \dots, L-1) \\ F_L &= -\sin(\theta_L) - \sin(\theta_L - \theta_{L-1}),\end{aligned}\tag{3}$$

where the friction coefficients γ_l and γ_h have been (for numerical convenience) chosen $\gamma_l = \gamma_h = 1$, and η_l and η_h are random Gaussian distributions with zero mean value and unit variance.

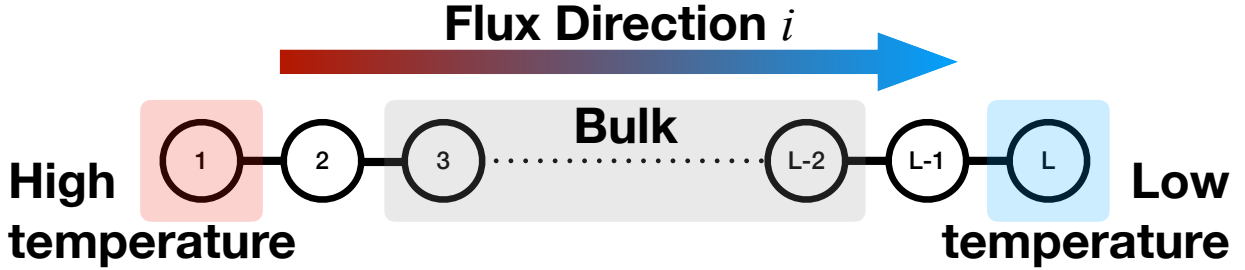


Figure 1: The lattice structure of the present $d = 1$ model (L sites).

For $d = 2$ (see Fig. 2):

$$\begin{aligned}\dot{\theta}_{i,j} &= p_{i,j} \quad ((i,j) = 1, \dots, L) \\ \dot{p}_{1,j} &= -\gamma_h p_{1,j} + F_{1,j} + \sqrt{2\gamma_h T_h} \eta_{j,h}(t) \\ \dot{p}_{i,j} &= F_{i,j} \quad (i = 2, \dots, L-1) \\ \dot{p}_{L,j} &= -\gamma_l p_{L,j} + F_{L,j} + \sqrt{2\gamma_l T_l} \eta_{j,l}(t),\end{aligned}\tag{4}$$

the force components being given by

$$\begin{aligned}F_{1,j} &= -\sin(\theta_{1,j} - \theta_{2,j}) - \sin(\theta_{1,j}) \\ &\quad - \sin(\theta_{1,j} - \theta_{1,j+1}) - \sin(\theta_{1,j} - \theta_{1,j-1}) \\ F_{i,j} &= -\sin(\theta_{i,j} - \theta_{i+1,j}) - \sin(\theta_{i,j} - \theta_{i-1,j}) \\ &\quad - \sin(\theta_{i,j} - \theta_{i,j+1}) - \sin(\theta_{i,j} - \theta_{i,j-1}) \\ F_{L,j} &= -\sin(\theta_{L,j}) - \sin(\theta_{L,j} - \theta_{L-1,j}) \\ &\quad - \sin(\theta_{L,j} - \theta_{L,j+1}) - \sin(\theta_{L,j} - \theta_{L,j-1}) \\ &\quad \text{with } \theta_{i,1} = \theta_{i,L+1} \text{ and } \theta_{i,0} = \theta_{i,L}.\end{aligned}\tag{5}$$

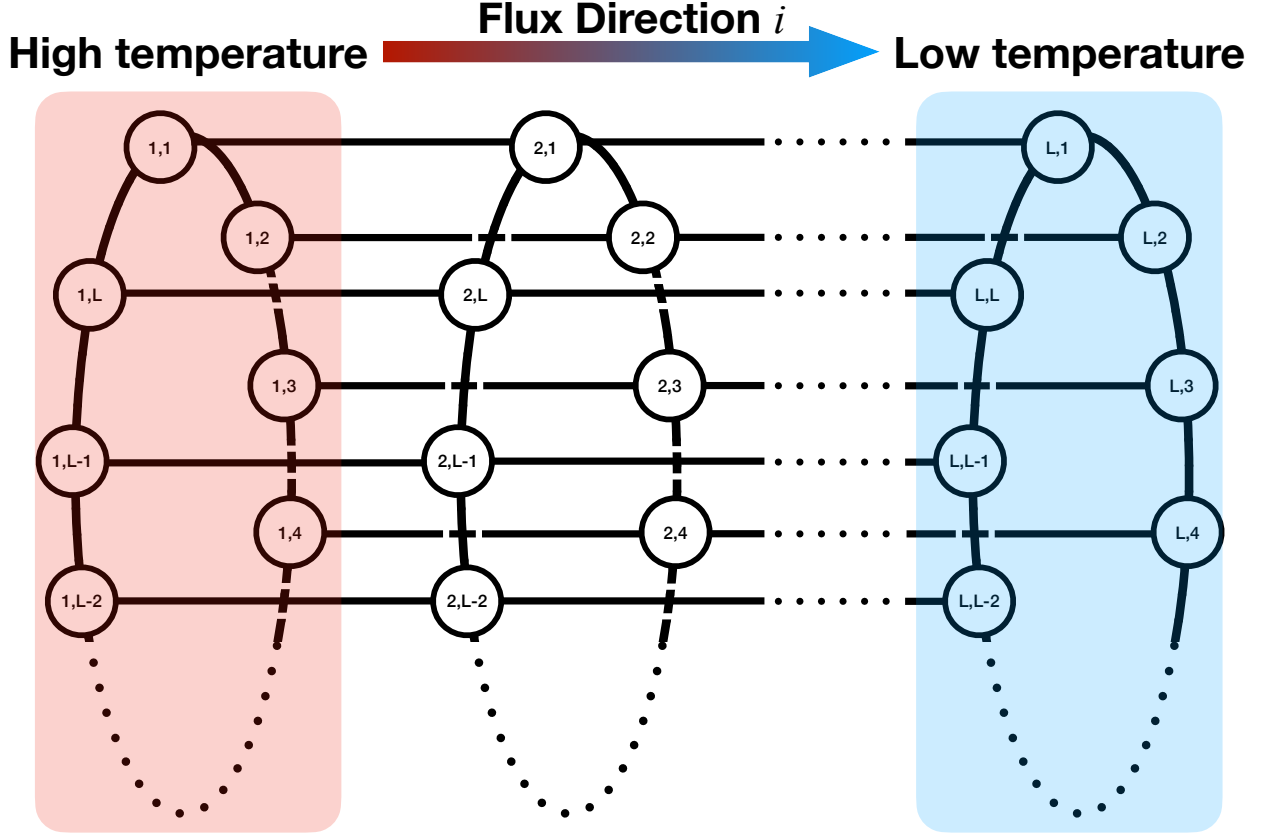


Figure 2: The lattice structure of the present $d = 2$ model (L^2 sites).

where the friction coefficients γ_l and γ_h have been chosen $\gamma_l = \gamma_h = 1$, and all components of the vectors $\eta_{j,l}$ and $\eta_{j,h}$ are random Gaussian distributions with zero mean value and unit variance.

For $d = 3$:

$$\begin{aligned}
 \dot{\theta}_{i,j,k} &= p_{i,j,k} \quad ((i, j, k) = 1, \dots, L) \\
 \dot{p}_{1,j,k} &= -\gamma_h p_{1,j,k} + F_{1,j,k} + \sqrt{2\gamma_h T_h} \eta_{j,k,h}(t) \\
 \dot{p}_{i,j,k} &= F_{i,j,k} \quad (i = 2, \dots, L-1) \\
 \dot{p}_{L,j,k} &= -\gamma_l p_{L,j,k} + F_{L,j,k} + \sqrt{2\gamma_l T_l} \eta_{j,k,l}(t),
 \end{aligned} \tag{6}$$

the force components being given by

$$\begin{aligned}
 F_{1,j,k} &= -\sin(\theta_{1,j,k} - \theta_{2,j,k}) - \sin(\theta_{1,j,k}) \\
 &\quad - \sin(\theta_{1,j,k} - \theta_{1,j+1,k}) - \sin(\theta_{1,j,k} - \theta_{1,j-1,k}) \\
 &\quad - \sin(\theta_{1,j,k} - \theta_{1,j,k+1}) - \sin(\theta_{1,j,k} - \theta_{1,j,k-1}) \\
 F_{i,j,k} &= -\sin(\theta_{i,j,k} - \theta_{i+1,j,k}) - \sin(\theta_{i,j,k} - \theta_{i-1,j,k}) \\
 &\quad - \sin(\theta_{i,j,k} - \theta_{i,j+1,k}) - \sin(\theta_{i,j,k} - \theta_{i,j-1,k}) \\
 &\quad - \sin(\theta_{i,j,k} - \theta_{i,j,k+1}) - \sin(\theta_{i,j,k} - \theta_{i,j,k-1}) \\
 F_{L,j,k} &= -\sin(\theta_{L,j,k}) - \sin(\theta_{L,j,k} - \theta_{L-1,j,k}) \\
 &\quad - \sin(\theta_{L,j,k} - \theta_{L,j+1,k}) - \sin(\theta_{L,j,k} - \theta_{L,j-1,k}) \\
 &\quad - \sin(\theta_{L,j,k} - \theta_{L,j,k+1}) - \sin(\theta_{L,j,k} - \theta_{L,j,k-1}) \\
 &\quad \text{with } \theta_{i,1,k} = \theta_{i,L+1,k}, \theta_{i,0,k} = \theta_{i,L,k}, \\
 &\quad \theta_{i,j,1} = \theta_{i,j,L+1} \text{ and } \theta_{i,j,0} = \theta_{i,j,L}.
 \end{aligned} \tag{7}$$

where the friction coefficients γ_l and γ_h have been chosen $\gamma_l = \gamma_h = 1$, and all components of the matrices $\eta_{j,k,l}$ and $\eta_{j,k,h}$ are random Gaussian distributions with zero mean value and unit variance.

The equations of the motion of N interacting rotors for any interaction topology can also be written in a compact form as follows:

$$\begin{aligned} \dot{\theta}_i &= p_i \\ \dot{p}_i &= \begin{cases} -\gamma_h p_i - \sin(\theta_i) - \sum_{j=1}^N A_{ij} \sin(\theta_i - \theta_j) + \sqrt{2\gamma_h T_h} \eta_i(t) & : i \in R_h \\ -\sum_{j=1}^N A_{ij} \sin(\theta_i - \theta_j) & : i \in R_b \\ -\gamma_c p_i - \sin(\theta_i) - \sum_{j=1}^N A_{ij} \sin(\theta_i - \theta_j) + \sqrt{2\gamma_c T_c} \mu_i(t) & : i \in R_l \end{cases} \end{aligned} \quad (8)$$

where $\mathbf{A} = [A_{ij}]$ is the topological interaction matrix, and R_h, R_b and R_l are the sets of rotors in the high-temperature heat bath, the bulk and the low-temperature heat bath, respectively. The associated lattice topology matrices, \mathbf{A} , we use in the current work for $d=1,2,3$ are detailed in Appendix.

Let us focus on the structure of the present d -dimensional systems. For $d = 1$, the system is simply an open chain of L sites, having at the ends two sites at temperatures T_h and T_l respectively. For $d = 2$, we have a three-dimensional hole cylinder as indicated in Fig. 2. In other words, we have L first-neighboring connected circles of L sites each, having at the two ends two circles at temperatures T_h and T_l respectively. Although the L sites of each of the ending circles are fixed at the same temperature, they obey independent random variables. For $d = 3$, we have a four-dimensional hole hyper-cylinder. In other words, we have L first-neighboring connected torus of L^2 sites each, having at the two ends two torus at temperatures T_h and T_l respectively. Although the L^2 sites of each of the ending torus are fixed at the same temperature, they obey independent random variables.

The dynamical evolution for the three cases ($d=1,2,3$) has been calculated through the Velocity Verlet algorithm [20, 21] with the stepsize $dt = 0.01$; after discarding a transient time, the average of the heat flux is realized for 4×10^8 time steps. The system is assumed to have reached the stationary state. For simplicity, we set $T_h = T(1 + \Delta)$ and $T_l = T(1 - \Delta)$ with $\Delta = 0.125$, where T is the average temperature defined above. The macroscopic conductivity κ is calculated by the following expression

$$\kappa = \frac{J}{(T_h - T_l)/L}. \quad (9)$$

where $J = \langle J_i \rangle$ is the time and space average heat flux along the bulk of the lattice in the stationary state. The bulk is defined as the entire system excluding the sides in high and low temperature heat baths and their first neighbors to avoid the direct effect of stochastic dynamics on the flux calculation. For the model with $d = 1$, the sides 1, 2, $(L - 1)$ and L were excluded to compute $\langle J_i \rangle$ (see Fig. 1). Similarly, the bulk is selected for the lattices with $d = 2$ and 3. Therefore, the possible minimum system length for any lattice topology L^d is $L = 5$ to compute the flow as desired. Furthermore, to reduce the direct effect of noise on the flux, one can ignore more than two nearest neighbors to the heat baths from the calculation for large systems. The time derivative of the Hamiltonian Eq. 1 can be written as

$$\frac{d\mathcal{H}}{dt} = -\frac{1}{2} \sum_{\ell=1}^{L^d} (J_\ell - J_{\ell'}) \quad (10)$$

where $J_\ell = (p_\ell + p_{\ell'}) \sin(\theta_\ell - \theta_{\ell'})$ is the Lagrangian flux [22], $\ell \in \{1, \dots, L^d\}$ is a unique label for each site and ℓ' is the nearest-neighbor of site- ℓ towards to hot reservoir. Therefore, J_ℓ is defined as the energy transfer per unit time, per transverse $(d - 1)$ -dimensional "area" L^{d-1} , i.e., per unit area L^2 for $d = 3$, per unit length L for $d = 2$, and without any unit for $d = 1$. Note that the calculation of J_ℓ is independent of the lattice dimension d since the direction of the flow is always in one direction from the hot end to the cold end. The statement for the flux direction is straightforward for $d = 1$; however, the model for $d > 1$ has periodic boundary conditions for interacting sides on $(d - 1)$ dimensions. Then the flux is defined only through the axis where the boundaries are closed with the heat baths in any lattice dimension $d \in \mathbb{Z}^+$. The macroscopic conductivity κ only depends on the specific material and its temperature. This is essentially the content of Fourier's 1822 law, where only the macroscopic phenomenon was focused on.

The (dimensionless) conductivity κ and the (dimensionless) "conductance" σ are, by definition, related through

$$\kappa \equiv \sigma L^d. \quad (11)$$

Table 1: Optimal fitting parameters $(A, q, B, \delta, \gamma, \eta)$. They have been obtained by focusing on the results corresponding to the largest computationally available values of L .

d	A	q	B	γ	δ	η	$\rho_\sigma = \gamma\eta/(q-1) + \delta$	$\rho_\kappa = \rho_\sigma - d$
1	0.191 ± 0.005	1.70 ± 0.05	0.60 ± 0.05	0.30 ± 0.03	0	2.36 ± 0.06	1.01 ± 0.06	0.01 ± 0.06
2	0.23 ± 0.05	3.4 ± 0.3	0.013 ± 0.002	0.40 ± 0.09	1	5.7 ± 0.5	1.95 ± 0.5	-0.05 ± 0.5
3	0.16 ± 0.05	3.2 ± 0.3	0.003 ± 0.002	0.45 ± 0.09	2	4.7 ± 0.5	2.96 ± 0.5	-0.04 ± 0.5

As we shall later on verify, this specific definition of σ has the advantage that, for $d = 1$ [16], σ does not depend on L in the $T \rightarrow 0$ limit.

In 2015 a numerical study showed [17], for the $d = 1$ first-neighbor planar-rotator model, the dependence on T of σ and κ for sizes L in the range [50, 1600] and a power-law was found at high temperatures. It was shown [16] two years later that all the available results can be collapsed, for L in the range [25, 2000] through the following q -Gaussian:

$$\sigma(T, L) = \sigma_0 e_q^{-B_q(L^{1/3}T)^2} \quad (12)$$

where, for $d = 1$, $\sigma_0 \equiv \sigma(0, L)$ depends from L , and $(q, B_q) \simeq (1.55, 0.40)$, the q -exponential function being defined as $e_q^z \equiv [1 + (1-q)z]^{1/(1-q)}$ ($e_1^z = e^z$). This function extremizes, under appropriate simple constraints, the nonadditive entropy [23, 24, 25]

$$\begin{aligned} S_q &\equiv k \frac{1 - \sum_i p_i^q}{q-1} = k \sum_i p_i \ln_q \frac{1}{p_i} \\ &= -k \sum_i p_i^q \ln_q p_i = -k \sum_i p_i \ln_{2-q} p_i \end{aligned} \quad (13)$$

where $\ln_q z \equiv \frac{z^{1-q} - 1}{1-q}$ ($\ln_1 z = \ln z$). We straightforwardly verify that $S_1 = S_{BG} \equiv -k \sum_i p_i \ln p_i$, where BG stands for Boltzmann-Gibbs. We also verify that, for two probabilistically independent systems A and B (i.e., $p_{ij}^{A+B} = p_i^A p_j^B$),

$$\frac{S_q(A+B)}{k} = \frac{S_q(A)}{k} + \frac{S_q(B)}{k} + (1-q) \frac{S_q(A)}{k} \frac{S_q(B)}{k}. \quad (14)$$

This property exhibits the nonadditivity of the entropic functional S_q for $q \neq 1$. For $q = 1$ we recover the well known additivity $S_{BG}(A+B) = S_{BG}(A) + S_{BG}(B)$.

We revisit here the $d = 1$ results of [16] by focusing higher values of T as well. It turns out that, while the q -Gaussian Ansatz was good enough for the conductivity σ at the relatively low temperatures considered in [16], the present numerics at a wider range of T (as well as those to be soon published [18]) require a more general Ansatz, namely the following stretched form q -exponential

$$y = e_q^{-B|x|^\eta} \quad (15)$$

with $q > 1$, $\eta > 2$ and $B > 0$. The q -Gaussian form is recovered as the $\eta = 2$ particular limit.

The present numerical results are indicated in Figs. 3, 4 and 5, where *trans*, *time* and *expr* denote the transient time necessary to achieve the stationary state, the time along which average is performed for a given experiment, and number of independent experiments which also are averaged, respectively (the most sensitive computational parameter is *trans*). All these results can be collapsed in the following universal form:

$$\sigma(T, L) L^{\delta(d)} = A(d) e_q^{-B(d)|T L^{\gamma(d)}|^{\eta(d)}} \quad (16)$$

The fitting parameters $(A, B, q, \eta, \gamma, \delta)$ are indicated in Table 1.

3 Conclusions

We summarize now the present research. The specific statistical mechanics correctly describing a given physical many-body problem depends on various aspects, which include the range of the interactions and the boundary conditions. The classical model that is being focused on here concerns short-range interactions. Therefore it constitutes a typical situation that, at thermal equilibrium, is correctly approached within the centennial BG theory (i.e., $q = 1$). This would naturally be the case if we had fully periodic boundary conditions, i.e., $T_h = T_l$. But the present non-equilibrium

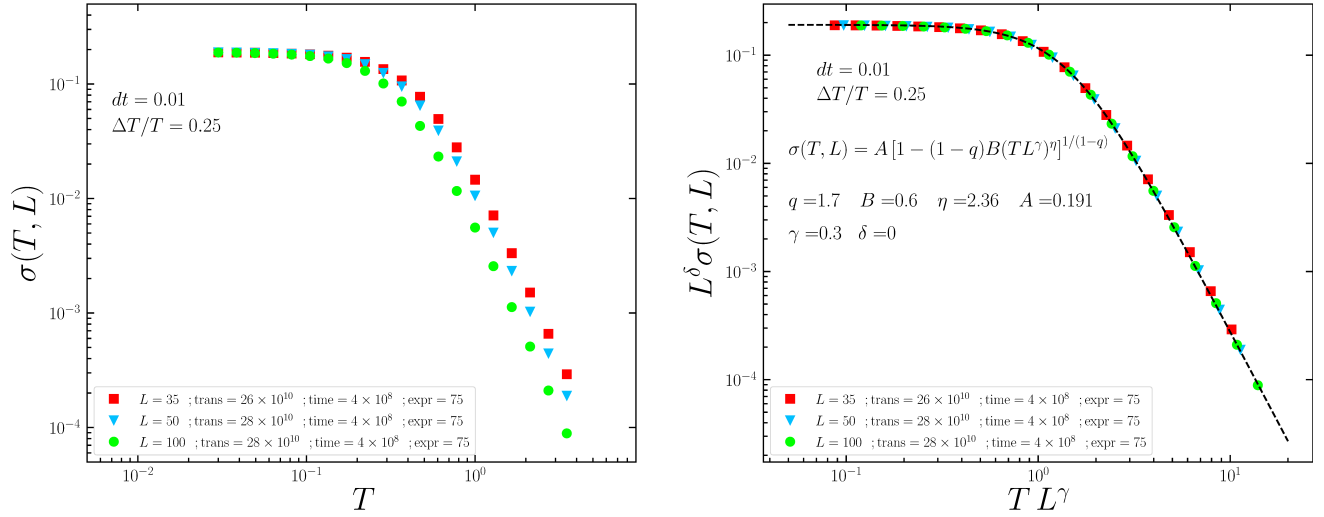


Figure 3: Case $d = 1$. *Left*: Conductivity for different sizes L . *Right*: Collapse of σ for all available sizes. The temperature T scales with the power L^γ . The $T \rightarrow 0$ value scales with L^δ . In the fitting, special attention has been paid to the large values of L .

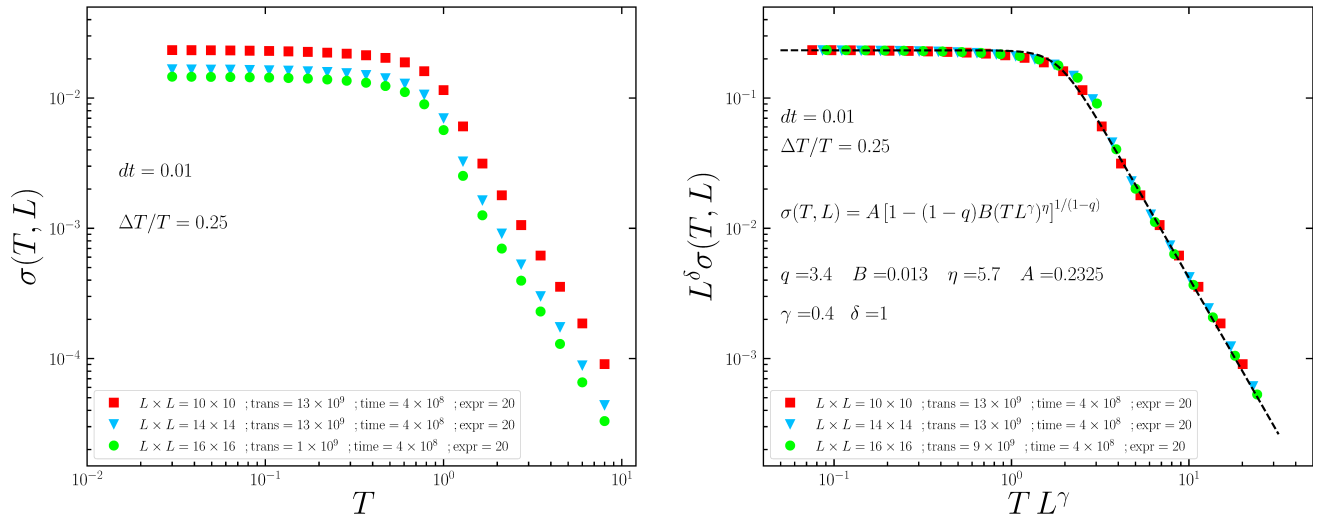


Figure 4: Case $d = 2$. *Left*: Conductivity for different sizes L . *Right*: Collapse of σ for all available sizes. The temperature T scales with the power L^γ . The $T \rightarrow 0$ value scales with L^δ . In the fitting, special attention has been paid to the large values of L .

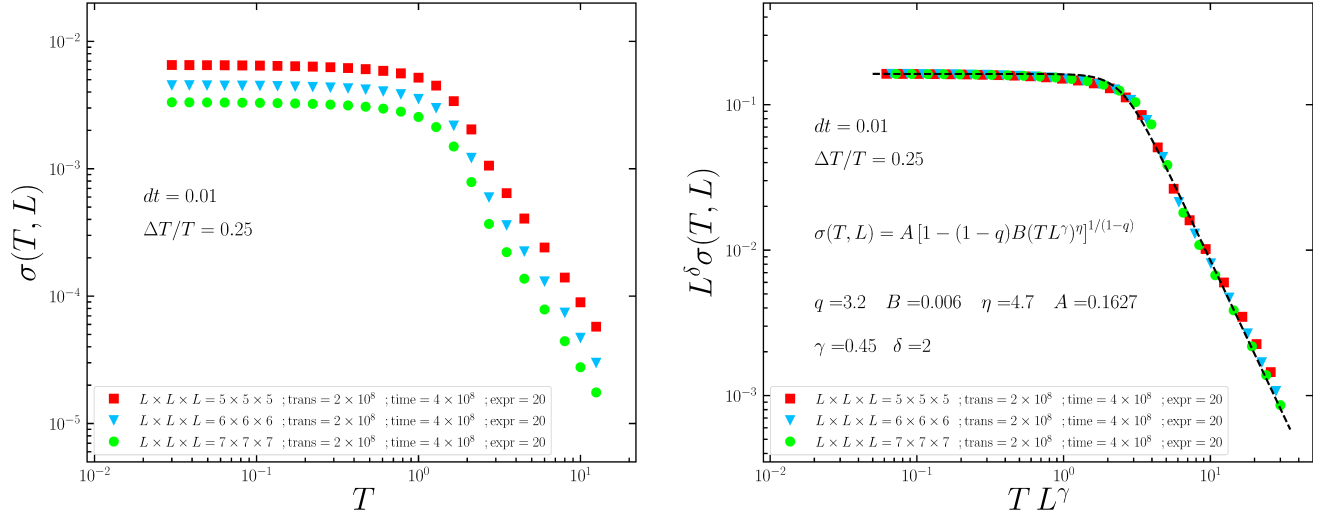


Figure 5: Case $d = 3$. *Left*: Conductivity for different sizes L . *Right*: Collapse of σ for all available sizes. The temperature T scales with the power L^γ . The $T \rightarrow 0$ value scales with L^δ . In the fitting, special attention has been paid to the large values of L .

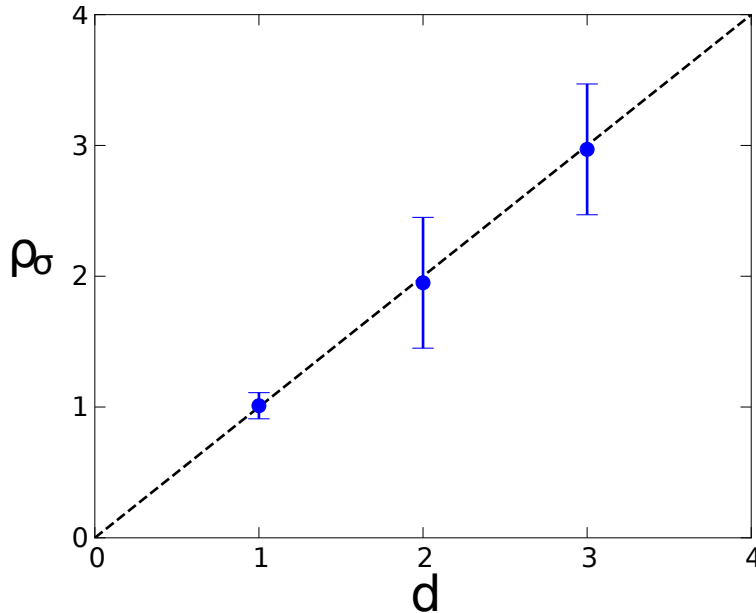


Figure 6: $\sigma \propto 1/L^{\rho_\sigma(d)}$ ($L \rightarrow \infty$) and $\kappa = \sigma L^d \propto L^{d-\rho_\sigma(d)}$. The dots correspond to the present numerical results (see Table 1). The dashed line indicates the validity of Fourier's law, i.e., $\lim_{L \rightarrow \infty} \kappa(T, L)$ is a finite T -dependent quantity. These results strongly suggest that $\rho_\sigma = d$, hence $\rho_\kappa = 0, \forall d$.

2D-Model: Cylinder Topology

The connectivity matrix, $\mathbf{A}_{\text{cylinder}}$, is $L^2 \times L^2$ matrix representing a 2-dimensional lattice system with periodic boundary conditions through one axis (cylinder shape), which is defined as follows:

$$\mathbf{A}_{\text{cylinder}} = \begin{bmatrix} \mathbf{A}_{\text{ring}} & \mathbf{I} & & & & & \\ \mathbf{I} & \mathbf{A}_{\text{ring}} & \mathbf{I} & & & & \mathbf{0} \\ & \mathbf{I} & \mathbf{A}_{\text{ring}} & \ddots & & & \\ & & \ddots & \ddots & \ddots & & \\ & & & \ddots & \ddots & \mathbf{I} & \\ & \mathbf{0} & & & \mathbf{I} & \mathbf{A}_{\text{ring}} & \mathbf{I} \\ & & & & \mathbf{I} & \mathbf{A}_{\text{ring}} & \end{bmatrix} \quad (18)$$

where \mathbf{I} is $L \times L$ identity matrix and \mathbf{A}_{ring} is $L \times L$ matrix as follows:

$$\mathbf{A}_{\text{ring}} = \begin{bmatrix} 0 & 1 & & & & & 1 \\ 1 & 0 & 1 & & & & \mathbf{0} \\ & 1 & 0 & \ddots & & & \\ & & \ddots & \ddots & \ddots & & \\ & & & \ddots & 1 & 0 & 1 \\ \mathbf{1} & \mathbf{0} & & & 1 & 0 & 0 \end{bmatrix} \quad (19)$$

3D-Model: Coupled-Tori Topology

The connectivity matrix, $\mathbf{A}_{\text{coupled-tori}}$, is $L^3 \times L^3$ matrix representing 3-dimensional coupled tori system, which is defined as follows:

$$\mathbf{A}_{\text{coupled-tori}} = \begin{bmatrix} \mathbf{A}_{\text{torus}} & \mathbf{I}_2 & & & & & \\ \mathbf{I}_2 & \mathbf{A}_{\text{torus}} & \mathbf{I}_2 & & & & \mathbf{0} \\ & \mathbf{I}_2 & \mathbf{A}_{\text{torus}} & \ddots & & & \\ & & \ddots & \ddots & \ddots & & \\ & & & \ddots & \ddots & \mathbf{I}_2 & \\ & \mathbf{0} & & & \mathbf{I}_2 & \mathbf{A}_{\text{torus}} & \mathbf{I}_2 \\ & & & & \mathbf{I}_2 & \mathbf{A}_{\text{torus}} & \end{bmatrix} \quad (20)$$

where \mathbf{I}_2 is $L^2 \times L^2$ identity matrix and $\mathbf{A}_{\text{torus}}$ is $L^2 \times L^2$ matrix as follows:

$$\mathbf{A}_{\text{torus}} = \begin{bmatrix} \mathbf{A}_{\text{ring}} & \mathbf{I} & & & & & \mathbf{I} \\ \mathbf{I} & \mathbf{A}_{\text{ring}} & \mathbf{I} & & & & \mathbf{0} \\ & \mathbf{I} & \mathbf{A}_{\text{ring}} & \ddots & & & \\ & & \ddots & \ddots & \ddots & & \\ & & & \ddots & \ddots & \mathbf{I} & \\ \mathbf{I} & \mathbf{0} & & & \mathbf{I} & \mathbf{A}_{\text{ring}} & \mathbf{I} \\ & & & & \mathbf{I} & \mathbf{A}_{\text{ring}} & \end{bmatrix}. \quad (21)$$

Acknowledgements

We acknowledge interesting remarks by E.P. Borges as well as partial financial support from CNPq and Faperj (Brazilian agencies). The numerical calculations reported in this paper were partially performed at TUBITAK ULAKBIM, High Performance and Grid Computing Center (TRUBA resources). U.T. is a member of the Science Academy, Bilim Akademisi, Turkey. D.E. was supported by the BAGEP Award of the Science Academy, Turkey.

References

- [1] J.B.J. Fourier, *Théorie analytique de la chaleur*, (Paris, Firmin Didot Père et Fils, 1822).
- [2] G.S. Ohm, *Die galvanische Kette, mathematisch bearbeitet*, (Berlin, T.H. Riemann, 1827).
- [3] A. Fick, *Ueber Diffusion*, *Annalen der Physik* **94** (1), 59-86 (1855).
- [4] S. Lepri, R. Livi and A. Politi, *Thermal conduction in classical low-dimensional lattices*, *Phys. Rep.* **377**, 1-80 (2003).
- [5] B. Li, G. Casati, J. Wang and T. Prosen, *Fourier law in the alternate-mass hard-core potential chain*, *Phys. Rev. Lett.* **92**, 254301 (2004).
- [6] C. Mejia-Monasterio, T. Prosen and G. Casati, *Fourier's law in a quantum spin chain and the onset of quantum chaos*, *Europhys. Lett.* **72** (4), 520-526 (2005).
- [7] N. Mingo and D.A. Broido, *Carbon nanotube ballistic thermal conductance and its limits*, *Phys. Rev. Lett.* **95**, 096105 (2005).
- [8] L. Yang, P. Grassberger and B. Hu, *Dimensional crossover of heat conduction in low dimensions*, *Phys. Rev. E* **74**, 062101 (2006).
- [9] A. Dhar, *Heat transport in low-dimensional systems*, *Advances in Physics* **57** (5), 457-537 (2008).
- [10] J.W. Jiang, J.S. Wang and B. Li, *Thermal conductance of graphene and dimerite*, *Phys. Rev. B* **79**, 205418 (2009).
- [11] S. Chen, J. Wang, G. Casati and G. Benenti, *Nonintegrability and the Fourier heat conduction law*, *Phys. Rev. E* **90**, 032134 (2014).
- [12] N. Yang, S. Hu, D. Ma, T. Lu and B. Li, *Nanoscale graphene disk: A natural functionally graded material—how is Fourier's law violated along radius direction of 2D disk*, *Scientific Reports* **5**, 14878 (2015).
- [13] N.Q. Le, C.A. Polanco, R. Rastgarkafshgarkolaei, J. Zhang, A.W. Ghosh and P.M. Norris, *Effects of bulk and interfacial anharmonicity on thermal conductance at solid/solid interfaces*, *Phys. Rev. B* **95**, 245417 (2017).
- [14] R. Luo, *Heat conduction in two-dimensional momentum-conserving and -nonconserving gases*, *Phys. Rev. E* **102**, 052104 (2020).
- [15] C. Zhang, D. Ma, M. Shang, X. Wan, J.T. Lü, Z. Guo, B. Li and N. Yang, *Violation of Fourier's law in homogeneous systems*, arxiv 1905.09183[cond-mat.mes-hall] (2021).
- [16] Y. Li, N. Li, U. Tirnakli, B. Li and C. Tsallis, *Thermal conductance of the coupled-rotator chain: Influence of temperature and size*, *EPL* **117**, 60004 (2017).
- [17] Y. Li, N. Li and B. Li, *Temperature dependence of thermal conductivities of coupled rotator lattice and the momentum diffusion in standard map*, *Eur. Phys. J. B* **88**, 182 (2015).
- [18] H.S. Lima, C. Tsallis, U. Tirnakli and D. Eroglu, *Fourier's law and the planar-rotator chain with generic-range coupling* (2022), in progress.
- [19] C. Olivares and C. Anteneodo, *Role of the range of the interactions in thermal conduction*. *Phys. Rev. E* **94**, 042117 (2016).
- [20] L. Verlet, *Computer "experiments" on classical fluids. I. Thermodynamical properties of Lennard-Jones molecules*, *Phys. Rev.* **159**, 98 (1967).
- [21] M.G. Paterlini and D.M. Ferguson, *Constant temperature simulations using the Langevin equation with velocity Verlet integration*, *Chemical Physics* **236**, 243-252 (1998).
- [22] C. Mejía-Monasterio, A. Politi and L. Rondoni, *Heat flux in one-dimensional systems*, *Phys. Rev. E* **100**, 032139 (2019).
- [23] C. Tsallis, *Possible generalization of Boltzmann-Gibbs statistics*, *J. Stat. Phys.* **52**, 479-487 (1988).
- [24] C. Tsallis, *Introduction to Nonextensive Statistical Mechanics – Approaching a Complex World* (Springer, New York, 2009); Second Edition (2022).
- [25] C. Tsallis, *Entropy*, *Encyclopedia* **2**, 264-300 (2022).